Imaging polarized granule release at the cytotoxic T cell immunological synapse using TIRF microscopy: control by polarity regulators

[1,2]Marie Juzans, [1]Céline Cuche, [1]Vincenzo Di Bartolo, [1]Andrés Alcover

[1]Institut Pasteur, Université de Paris, INSERM-U1224, Unité Biologie Cellulaire des Lymphocytes, Ligue Nationale Contre le Cancer, Équipe Labellisée Ligue-2018. F-75015 Paris, France

Corresponding author's email address: andres.alcover@pasteur.fr

[2] MJ present address: Department of Pathology and Laboratory Medicine, Children's Hospital of Philadelphia Research Institute, Perelman School of Medicine at the University of Pennsylvania, Philadelphia, PA, USA.

Outline

Abstract

Immunological synapse formation results from a profound T cell polarization process that involves the coordinated action of the actin and microtubule cytoskeleton, and the intracellular traffic of several vesicular organelles. T cell polarization is key for both T cell activation leading to T cell proliferation and differentiation, and for T cell effector functions such as polarized secretion of cytokines by helper T cells, or polarized delivery of lytic granules by cytotoxic T cells. Efficient targeting of lytic granules by cytotoxic T cells is a crucial event for the control and elimination of infected or tumor cells. Understanding how lytic granule delivery is regulated and quantifying its efficiency under physiological and pathological conditions may help to improve immune responses against infection and cancer.

1 Introduction

Immunological synapse structure and function depends on a complex process of T cell polarization towards antigen presenting cells or target cells. Polarization is initiated by T cell receptor (TCR) engagement and occurs as the result of the reorganization of both the actin and microtubule cytoskeleton, resulting in the translocation of several organelles to the antigen-presenting cell contact site. These include the Golgi apparatus, and the endosomal and lysosomal compartments that reorient their intracellular vesicle traffic towards the immunological synapse. T cell polarization depends on TCR signal transduction and involves an array of signaling, cytoskeleton and vesicle traffic regulators (Mastrogiovanni et al., 2020). Cytotoxic T lymphocyte (CTL) effector function depends on the appropriate delivery of lytic granules to the plasma membrane and on their fusion at the zone of contact with target cells. Lytic granules are part of the late endosomal/lysosomal compartment. Molecular motors and intracellular traffic regulators allow lytic granule transport, docking and fusion with the plasma membrane and the delivery of their components, such as perforin and granzymes, to target cells provoking their death (de Saint Basile et al., 2010). Centrosome polarization and docking to the immunological synapse, and actin polymerization and clearance from the center of the contact site have been proposed to facilitate the formation of a secretory domain allowing optimal lytic granule delivery and fusion at the CTL-target cell contact (Randzavola et al., 2019; Ritter et al., 2015; Stinchcombe et al., 2001; Stinchcombe et al., 2006). However, this seems not to be the sole mechanism (Bertrand et al., 2013; Tamzalit et al., 2020). Conversely, actin recovery at the center of the immunological synapse is associated with termination of lytic granule release (Ritter et al., 2017). Defects in regulators of vesicle traffic or cytoskeleton dynamics are associated with defects in CTL function and immunodeficiency (de Saint Basile et al., 2010).

The role of cell polarity regulators in this process has been recently unveiled (Juzans et al., 2020). Cell polarity regulators are scaffold proteins, endowed with a variety of protein-protein interaction motifs, whose effectors are involved in mechanisms controlling cytoskeleton organization, cell shape and symmetry. Several polarity regulators have been involved in T lymphocyte processes, including cell migration and immunological synapse formation (Mastrogiovanni et al., 2021). Among them, *Discs large homolog 1* (Dlg1) and *Adenomatous polyposis coli* (Apc) play key roles in immunological synapse formation and function in CD4 and CD8 T cells, *via* their control of microtubule network organization at the synapse (Aguera-Gonzalez et al., 2017; Juzans et al., 2020; Lasserre et al., 2010). The protocols we describe here were developed to investigate the involvement of the polarity regulator and tumor suppressor Apc in CTL polarized secretion of lytic granules. In order to have accurate imaging of granule dynamics and fusion, CTLs were induced to polarize on coverslips coated with anti-CD3 antibody. This is a previously described method that generates flat and spread two-dimensional pseudo-immunological synapses on which accurate microscopy imaging may be performed (Bunnell et al., 2003). We have shown before that these synapse structures clearly display finely organized microtubule networks and centrosome polarization (Aguera-Gonzalez et al., 2017; Juzans et al., 2020). To further ensure accurate visualization of granule docking and fusing at the plasma membrane, we used total internal reflection fluorescence (TIRF) microscopy.

TIRF microscopy uses a specific mode of sample illumination to exclusively excite fluorophores near the adherent cell surface (within ~100 nm), corresponding in our case to the plasma membrane at the pseudo synapse. This illumination mode is based on an evanescent wave produced when light rays are totally internally reflected at the interface between the cover glass and the adhered cell plasma membrane (Poulter et al., 2015). Since this illumination wave does not propagate deeply into the cell, the region imaged corresponds to the CTL plasma membrane where lytic granules are expected to dock and fuse. It prevents the overlap of images corresponding to granules located deeper inside the cell that would be visualized with other microcopy approaches as scanning or spinning disk confocal microscopy. Therefore, TIRF microscopy allows to differentiate granule polarization defects and docking/fusing defects.

2. Materials

2.1. Equipment

1. Cell culture incubator allowing standard cell culture conditions in a humidified atmosphere (37°C, 5% CO_2).

2. Standard bench top centrifuge (Eppendorf Centrifuge 5810R or 5415R).
3. Sterile cell culture laminar flow hood safety level II.
4. MACS MultiStand™ (Miltenyi Biotec, No 130-042-303).
5. MidiMACS™ Separator (Miltenyi Biotec, No 130-042-302).
6. Biosafety class 2 laboratory (BSL2 or P2).
7. Microscope: LSM 780 Elyra PS.1 confocal microscope (Zeiss) equipped with a TIRF module and a temperature and CO_2 controlled chamber. Images were acquired with a Plan-Apochromat 100x/1.46 numerical aperture oil immersion objective and the ZEN software (Zeiss).
8. ImageJ software with the TrackMate plugin (Tinevez et al., 2017).
9. MACSQuant® Analyzer flow cytometer (Miltenyi Biotec).
10. FlowJo v10 software (FlowJo, LLC) for flow cytometry data analysis.

2.2. Disposable materials

1. 24-well plates for cell culture (Falcon, No 353047).
2. μ-Dish 35 mm, high glass bottom (Ibidi, No 81158 or MatTek No P35G-1.5-10-C) (see **Note 1**).
3. Sterile microcentrifuge tubes (Eppendorf No 3810).
4. 96-well plates for cell culture (TPP, No 92097).

2.3. Chemicals and biological products

1. Lymphocyte Separating Medium Pancoll Human tubes (Pan Biotech, No P04-60125).
2. Magnetic cell sorting CD8+ T cell isolation kit (Miltenyi Biotec, No 130-096-495).
3. LS columns for magnetic cell sorting (Miltenyi Biotec, No 130-042-401).
4. MACS™ MultiStand (Miltenyi Biotec, No 130-042-303).
5. MidiMACS™ Separator (Miltenyi Biotec, No 130-042-302).
6. RPMI 1640 cell culture medium containing GlutaMAX-I and Phenol Red (Gibco, ThermoFisher Scientific, No 61870).
7. Sodium pyruvate (Life Technologies, No 11360).
8. Nonessential amino acids (Life Technologies, No 11140).
9. HEPES (N-(2-Hydroxyethyl)piperazine-N′-(2-ethanesulfonic acid) (Life Technologies, No 15630-056).
10. Penicillin–streptomycin (Gibco, No 15140-122).

11. Human serum (Dominique Dutscher, No S4190-100).
12. Fetal bovine serum (FBS): HyClone™ SERUM - Research grade fetal bovine serum, origin South America (Dominique Dutscher, No SV30160.03).
13. Purified anti-human CD3ε antibody, clone UCHT1 (BioLegend Inc, No 300402).
14. Anti-human CD28 antibody (Beckman Coulter, No IM1376).
15. Recombinant human IL-2 (PeproTech, No 200-02).
16. Dulbecco's PBS - Modified, w/o $CaCl_2$ and $MgCl_2$ (DPBS), (Gibco, ThermoFisher Scientific, No 14190).
17. Lentiviruses expressing short harpin RNAs (shRNAs) were obtained from (Sigma-Aldrich) (see **Note 2**).
18. Puromycin (Gibco, No A11138-03).
19. Bovine serum albumin (BSA) (Alpha Diagnostics, No 80400-100).
20. Fixable Viability Stain 450 (BD Biosciences).
21. Antibody cocktail-1 for T cell differentiation: anti-CD3-PE-Cy5 (1/30; clone HIT3a; BD Biosciences), anti-CD8-APC-Cy7 (1/30; clone RPA-T8; Biolegend), anti-CD25-Alexa fluor 488 (1/30; clone M-A251; Biolegend), anti-CD45RA-APC (1/30; cloneHI100; Biolegend), anti-CCR7-PE (1/50; clone G043H7; Biolegend).
22. Saponin (Sigma, No S7900).
23. Antibody cocktail-2 for granzyme B expression: anti-CD3-PE-Cy5 (1/30; clone HIT3a; BD Biosciences), anti-CD8-APC-Cy7 (1/30; clone RPA-T8; Biolegend).
24. Anti-Granzyme-B-PE antibody (1/50; clone GB12; Invitrogen).
25. HCl 1N (Fluka, No. 84436) solution in 70% ethanol (Fisher Chemical No E/0550DF/21).
26. Poly-L-lysine solution 0.1% (w/v) (Sigma-Aldrich, No P8920).
27. LysoTracker™ Deep Red (Invitrogen, No L12492) to label cytotoxic granules.
28. 5-Carboxyfluorescein diacetate (CFSE) (eBioscience No 65-0850) (see **Note 3**) to label cells.
29. RPMI 1640 medium, no phenol red (Gibco, ThermoFisher Scientific, No 11835).

3. Methods

Figure 1 shows the graphic summary of the methodology described below.

3.1. Primary $C8^+$ T cell isolation, differentiation, and lentiviral infection

3.1.1. Peripheral blood mononuclear cell (PBMC) isolation

Peripheral blood from healthy donors was obtained from the French National Blood Bank (*Etablissement Français du Sang*) using ethically approved procedures. PBMC were obtained by density gradient centrifugation using Lymphocyte Separating Medium Pancoll Human (see **Note 4**).

3.1.2. $CD8^+$ T cell isolation by magnetic cell sorting

Isolate $CD8^+$ T cells from PBMC by negative selection using magnetic cell sorting using a $CD8^+$ T Cell Isolation Kit and LS columns, following manufacturer's instruction.

Culture purified cells in RPMI 1640 cell culture medium supplemented with 10% FBS, 1 mM sodium pyruvate, 1% (v/v) nonessential amino acids, 10 mM HEPES, 0.5% (v/v) penicillin–streptomycin.

3.1.3. $CD8^+$ T cell activation and differentiation into CTLs

1. Coat 24-well plates with 400 µL human anti-CD3 (10 mg/mL) in PBS overnight at 4°C or 3 h at 37°C.
2. Wash plates 3 times with PBS, then incubate 1h at 37°C with 500 µL culture medium to prevent non-specific cell binding.
3. Resuspend freshly isolated $CD8^+$ T cells at 2.10^6 cell/mL in culture medium containing 7 mg/mL anti-CD28 (note that anti-CD28 is used soluble, whereas anti-CD3 is coated to the plate) and 100 U/mL recombinant human IL-2, remove medium from plates and distribute 500 µL of cell suspension in each well, incubate plates at 37°C with 5% CO_2 for 2 days (infection) or 6 days (FACS analysis). For FACS analysis, the concentration is adjusted to 2.10^6 cell/mL in culture medium containing 100 U/mL recombinant human IL-2 at day 2 and 4.

3.1.4. Assess CTL differentiation by FACS analysis

1. Take $0.5x10^6$ $CD8^+$ T cells at day 0-2-4-6 and place them in a 96 well plate.
2. Wash cells twice with PBS, centrifuge plates for 6 min at 450 x g remove supernatant and add 100 µL of PBS 1X with Fixable Viability Stain 450 (250 ng/mL; BD) diluted 1/1000 (v/v), incubate 10 min at RT.

3. Wash cells twice with PBS, 0.5% (w/v) BSA, spin plates for 6 min at 450 x g, remove supernatant and add 75 µL of PBS, 0.5% BSA with antibody cocktail-1 or -2, incubate 30 min at 4°C.
4. Wash cells twice with PBS, 0.5% BSA, spin plates for 6 min at 450 x g, remove supernatant.
5. Fix samples with antibody cocktail-1 by adding 200 µL of PBS, 0.5% BSA, 1% (w/v) paraformaldehyde (PFA), store at 4°C till flow cytometry analysis (see **point 10**).
6. Fix samples with antibody cocktail-2 by adding 100 µL of 4% PFA, incubate 15 min at RT.
7. Wash cells twice with PBS, 0.5% BSA, spin plates for 6 min at 450 x g, remove supernatant and add 60 µL of PBS, 0.5% BSA, 0.05% saponin to permeabilize cell membrane, incubate 10 min at RT.
8. Without wash add 15 µl of anti-Granzyme-B-PE (1/10 v/v; clone GB12; Invitrogen), incubate 30 min at 4°C.
9. Wash cells twice with PBS, 0.5% BSA, spin plates for 6 min at 450 x g, remove supernatant, add 200 µL of PBS, 0.5% BSA, 1% PFA.
10. Analyze samples by flow cytometry. In our case, samples were acquired with a MACSQuant® Analyzer and analyzed using FlowJo v10 software. All samples were gated on forward and side scatter (FSC/SSC), for single cells, and live cells. An example of the FACS gating procedure and typical results are shown in figure 2.

3.1.5. $CD8^+$ T cell lentiviral infection to generate silenced CTLs

1. After 2-day activation in 24-well plates, infect cells with lentiviruses in a P2 laboratory. Spin plates and remove supernatant, add 900 µL of culture medium in which FBS is replaced by 10% human serum (see **Note 5**), supplemented with 100 U/mL IL-2, add 100 µL of lentiviruses (see **Note 6**). In our case, these were coding for control or Apc-specific shRNAs. Incubate at 37°C with 5% CO_2 for 24 h.
2. Wash cells 3 times (see **Note 6**) by spinning plates for 7 min at 450 x g, remove supernatant, add 1 mL of fresh culture medium. Repeat twice with medium supplemented with 100 U/mL IL-2 and 3.9 mg/mL puromycin. Cells can be taken out of the P2 laboratory. Incubate at 37°C with 5% CO_2 for 3 days for selection.

3. The night before use, wash cells to remove dead cells. Spin plates for 7 min at 450 x g, remove supernatant, add 1 mL of fresh culture medium with 100 U/mL IL-2 without puromycin.

3.2. Imaging granule secretion by TIRF microscopy

3.2.1. Coat glass-bottom dishes with anti-CD3 antibody

1. Wash glass-bottom dishes with HCl-EtOH 70% for 10 min, rinse twice with water and once with EtOH 70% before letting them dry.
2. Coat glass-bottom dishes with poly-L-lysine at 0.002% (w/v) in water for 30 min at room temperature, wash once with water, let them dry (see **Note 7**).
3. Coat poly-L-lysine-coated dishes with anti-CD3 antibody at 10 mg/mL in PBS 3 h at 37°C or overnight at 4°C, wash 3 times with PBS, incubate 1 h at 37°C with culture medium to prevent cell non-specific binding (see **Note 7**).

3.2.2. Microscopy

1. Turn on the TIRF microscope, set up chamber temperature at 37°C, 5% CO_2 (see **Note 8**). Let the chamber equilibrate for at least one hour.
2. Collect CTLs by pulling several wells of cells infected with control or silencing lentivirus, wash wells twice with PBS.
3. Wash cells twice with PBS to remove dead cells, spin 7 min at 450 x g, resuspend at 1.10^6 cells/mL in PBS with 1µM CFSE, incubate 5 min at room temperature protected from light.
4. Wash cells twice with PBS, resuspend at 2.10^6 cells/mL in culture medium with 0.1 mM LysoTracker Deep Red, incubate 1 h at 37°C.
5. Wash cells twice with warm RPMI 1640 without phenol red, resuspend at $1.5x10^6$ cells/mL.
6. Equilibrate cells and glass-bottom dishes temperature in the microscope chamber for at least 15 min.
7. Remove medium from one dish, place it on the objective, add 100 µL of cell solution.
8. Follow CTL sedimentation using epifluorescence mode. Once cells reach the dish bottom, switch to TIRF mode to follow their spreading on anti-CD3 antibodies.
9. Start imaging when CTLs are spreading on the surface (pseudo-immunological synapse) (Figure 2 A, middle panel), acquire images in the TIRF plane every 150 ms for 5 min.

10. Repeat steps 7 to 9 for each image needed. Do not image twice the same dish to prevent acquiring CTLs that have already degranulated.

3.3. Quantitative image analysis

Granule total number and movement are quantified using the TrackMate plugin for ImageJ software (Tinevez et al., 2017), as shown in figure 3 and in reference (Juzans et al., 2020). This open-source plugin allows automated particle tracking. Granules are detected in individual cells based on their estimated diameter (0.5 μm approximately). Individual granule position is detected at each time point, allowing the automated linking between positions and missing detection filling. We recommend to set the maximum gap-closing frame on 1 to avoid linking detection between two different granules. Generated Excel files provide the number of granules present in the TIRF zone and their LysoTracker mean intensity at each time point. We recommend to consider only strongly fluorescent granules, more likely closer to the plasma membrane. To do so, a threshold of at least 2x the mean granule fluorescence intensity obtained for an experiment can be set. Granules that are never reaching this threshold are not included in the analysis. Files named Track Statistics also provide tracking duration for each granule, their mean speed during the tracking, and their displacement length (Figure 3 B-C-D). In addition, files named Spots in Track Statistics provides granule positions (x, y) at each time point allowing to study their directionality. Finally, fusion events are quantified by counting the fluorescence bursts for each cell (Figure 3 E-F).

4. Concluding remarks

The methodology described here allows to measure in a precise and quantitative manner the polarized secretion of granules in human *ex vivo*-differentiated CTLs. It has been applied to compare control and Apc-silenced cells, unveiling a regulatory control of the Apc polarity regulator and tumor suppressor in CTL effector function. It could be therefore applied to the investigation of other genes, or to the comparison of T cells from patients *versus* healthy subjects. Although very precise and quantitative, this methodology only allows the analysis of a restricted number of cells per experiment. This reduces the number of experimental conditions that can be investigated per experiment. Investigation of larger sample panels would need different microscopy set ups.

It is worth noting that we used LysoTracker to monitor lytic granule dynamics. This is a marker of late endosomal and lysosomal compartment, which includes lytic granules, but it is not fully specific for them. Alternative strategies have included the use of fluorescent protein-tagged

granzyme B or perforin, both components of lytic granules, see for instance (Pattu et al., 2013; Qu et al., 2011). However, this requires cell infection with lentiviral vectors expressing one of these proteins and would result in their overexpression. Furthermore, full activity or specific localization of these exogenous proteins will not be fully guaranteed.

5. Notes

1. Manipulate glass bottom dishes carefully and avoid putting them directly on the bench. Place them on Kimwipes (Kimtech Science) to avoid scratches on the coverslip.
2. Lentiviruses are produced by transiently transfecting HEK293T cells with the calcium phosphate DNA precipitation technique, as described elsewhere (Kwon and Firestein, 2013). The procedure is based on slow mixing HEPES-buffered saline containing sodium phosphate with a $CaCl_2$ solution containing the DNA. A DNA-calcium phosphate co-precipitate forms, which adheres to the cell surface and is taken up by the cell, presumably by endocytosis. Cells are transfected with pCMV-deltaR8-2, pCMV-env-VSV, and a pLKO.1- puro-CMV-tGFP lentiviral vector expressing or not (as negative control) a shRNA–targeting Apc (5'-GACTGTCCTTTCACCATATTT-3') (Sigma-Aldrich). After 48 h, supernatants are recovered, filtered, and concentrated 40x by ultracentrifugation (26,000 rpm or 11,3000 x g, 1.5 h, 4°C). Lentivirus stocks are then stored at -80°C.
3. This reagent is used to visualize cells under the microscope when lentiviral vectors do not contain a fluorescent tag (e.g. GFP). We strongly recommend the use of a fluorescent tag as it allows to identified transduced cells and analyze those with similar fluorescent intensity, reflecting similar lentiviral load.
4. Bring tubes containing the Human Lymphocyte Separating Medium Pancoll to room temperature. Pour carefully 30 mL of blood into each tube. Centrifuge at 800 x g for 30 min in a centrifuge with a swing-out rotor and brake switched off. Harvest the PBMC fraction between the plasma and the Pancoll with a pipette as depicted in the manufacturer's instructions. The membrane present in the tubes prevents contamination with granulocytes and erythrocytes. Wash twice the lymphocytes/PBMCs with DPBS, spin 10 min at 450 x g.
5. The use of human serum instead of fetal calf serum strongly increases cell transduction efficiency and cell viability of infected T cells.

6. It is very important not to change plates or even take the cells out during incubation time needed for lentiviral infection, as it will drastically reduce cell transduction efficiency and cell viability. Please note that the biosafety laboratory rules may change with the type of lentivirus used.
7. Glass-bottom dishes can be washed and coated with poly-L-lysine up to a week in advance. However, it is better to coat them with anti-CD3 antibody the day of the experiment.
8. If the microscope is not equipped with a CO_2 chamber, CO_2 independent Leibovitz's L-15 medium, without phenol red (Gibco, ThermoFisher Scientific, No 21083027) supplemented with 2 mg/mL D-glucose may be used.

Acknowledgements

This work was supported by a grant from La Ligue Contre le Cancer Equipe Labellisée Ligue-2018 and Institutional grants from Institut Pasteur and INSERM. MJ has been funded by an Allocation de Recherche Doctorale from La Ligue Nationale Contre le Cancer.

Declaration of Interests

The authors have no financial conflict of interest.

References

Aguera-Gonzalez, S., Burton, O.T., Vazquez-Chavez, E., Cuche, C., Herit, F., Bouchet, J., Lasserre, R., Del Rio-Iniguez, I., Di Bartolo, V., and Alcover, A. (2017). Adenomatous Polyposis Coli Defines Treg Differentiation and Anti-inflammatory Function through Microtubule-Mediated NFAT Localization. Cell Rep *21*, 181-194.

Bertrand, F., Muller, S., Roh, K.H., Laurent, C., Dupre, L., and Valitutti, S. (2013). An initial and rapid step of lytic granule secretion precedes microtubule organizing center polarization at the cytotoxic T lymphocyte/target cell synapse. Proc Natl Acad Sci U S A *110*, 6073-6078.

Bunnell, S.C., Barr, V.A., Fuller, C.L., and Samelson, L.E. (2003). High-resolution multicolor imaging of dynamic signaling complexes in T cells stimulated by planar substrates. Sci STKE *2003*, PL8.

de Saint Basile, G., Menasche, G., and Fischer, A. (2010). Molecular mechanisms of biogenesis and exocytosis of cytotoxic granules. Nat Rev Immunol *10*, 568-579.

Juzans, M., Cuche, C., Rose, T., Mastrogiovanni, M., Bochet, P., Di Bartolo, V., and Alcover, A. (2020). Adenomatous Polyposis Coli Modulates Actin and Microtubule Cytoskeleton at the Immunological Synapse to Tune CTL Functions. Immunohorizons *4*, 363-381.

Kwon, M., and Firestein, B.L. (2013). DNA transfection: calcium phosphate method. Methods in molecular biology *1018*, 107-110.

Lasserre, R., Charrin, S., Cuche, C., Danckaert, A., Thoulouze, M.I., de Chaumont, F., Duong, T., Perrault, N., Varin-Blank, N., Olivo-Marin, J.C*., et al.* (2010). Ezrin tunes T-cell activation by controlling Dlg1 and microtubule positioning at the immunological synapse. EMBO J *29*, 2301-2314.

Mastrogiovanni, M., Di Bartolo, V., and Alcover, A. (2021). Cell Polarity Regulators, Multifunctional Organizers of Lymphocyte Activation and Function. Biomed J.

Mastrogiovanni, M., Juzans, M., Alcover, A., and Di Bartolo, V. (2020). Coordinating Cytoskeleton and Molecular Traffic in T Cell Migration, Activation, and Effector Functions. Front Cell Dev Biol *8*, 591348.

Pattu, V., Halimani, M., Ming, M., Schirra, C., Hahn, U., Bzeih, H., Chang, H.F., Weins, L., Krause, E., and Rettig, J. (2013). In the crosshairs: investigating lytic granules by high-resolution microscopy and electrophysiology. Front Immunol *4*, 411.

Poulter, N.S., Pitkeathly, W.T., Smith, P.J., and Rappoport, J.Z. (2015). The physical basis of total internal reflection fluorescence (TIRF) microscopy and its cellular applications. Methods in molecular biology *1251*, 1-23.

Qu, B., Pattu, V., Junker, C., Schwarz, E.C., Bhat, S.S., Kummerow, C., Marshall, M., Matti, U., Neumann, F., Pfreundschuh, M.*, et al.* (2011). Docking of lytic granules at the immunological synapse in human CTL requires Vti1b-dependent pairing with CD3 endosomes. J Immunol *186*, 6894-6904.

Randzavola, L.O., Strege, K., Juzans, M., Asano, Y., Stinchcombe, J.C., Gawden-Bone, C.M., Seaman, M.N., Kuijpers, T.W., and Griffiths, G.M. (2019). Loss of ARPC1B impairs cytotoxic T lymphocyte maintenance and cytolytic activity. J Clin Invest *129*, 5600-5614.

Ritter, A.T., Asano, Y., Stinchcombe, J.C., Dieckmann, N.M., Chen, B.C., Gawden-Bone, C., van Engelenburg, S., Legant, W., Gao, L., Davidson, M.W.*, et al.* (2015). Actin depletion initiates events leading to granule secretion at the immunological synapse. Immunity *42*, 864-876.

Ritter, A.T., Kapnick, S.M., Murugesan, S., Schwartzberg, P.L., Griffiths, G.M., and Lippincott-Schwartz, J. (2017). Cortical actin recovery at the immunological synapse leads to termination of lytic granule secretion in cytotoxic T lymphocytes. Proc Natl Acad Sci U S A *114*, E6585-E6594.

Stinchcombe, J.C., Bossi, G., Booth, S., and Griffiths, G.M. (2001). The immunological synapse of CTL contains a secretory domain and membrane bridges. Immunity *15*, 751-761.

Stinchcombe, J.C., Majorovits, E., Bossi, G., Fuller, S., and Griffiths, G.M. (2006). Centrosome polarization delivers secretory granules to the immunological synapse. Nature *443*, 462-465.

Tamzalit, F., Tran, D., Jin, W., Boyko, V., Bazzi, H., Kepecs, A., Kam, L.C., Anderson, K.V., and Huse, M. (2020). Centrioles control the capacity, but not the specificity, of cytotoxic T cell killing. Proc Natl Acad Sci U S A *117*, 4310-4319.

Tinevez, J.Y., Perry, N., Schindelin, J., Hoopes, G.M., Reynolds, G.D., Laplantine, E., Bednarek, S.Y., Shorte, S.L., and Eliceiri, K.W. (2017). TrackMate: An open and extensible platform for single-particle tracking. Methods *115*, 80-90.

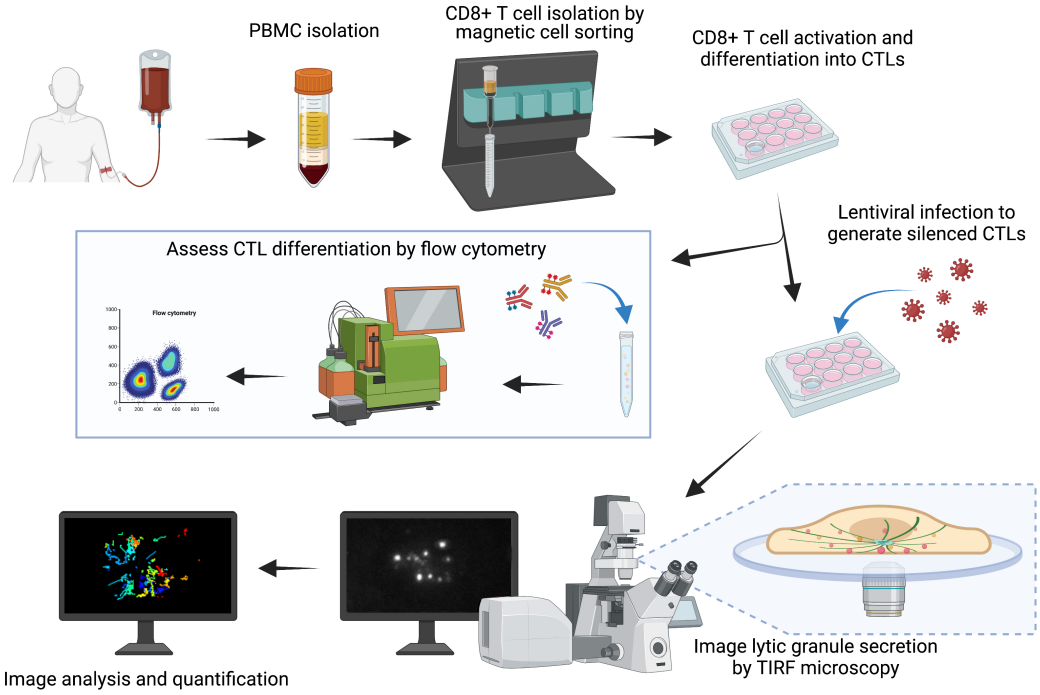

Figure 1. Graphic summary of the methodology described.
Work flow describing the different experimental steps involved in the procedures described in this chapter. Created with BioRender.com

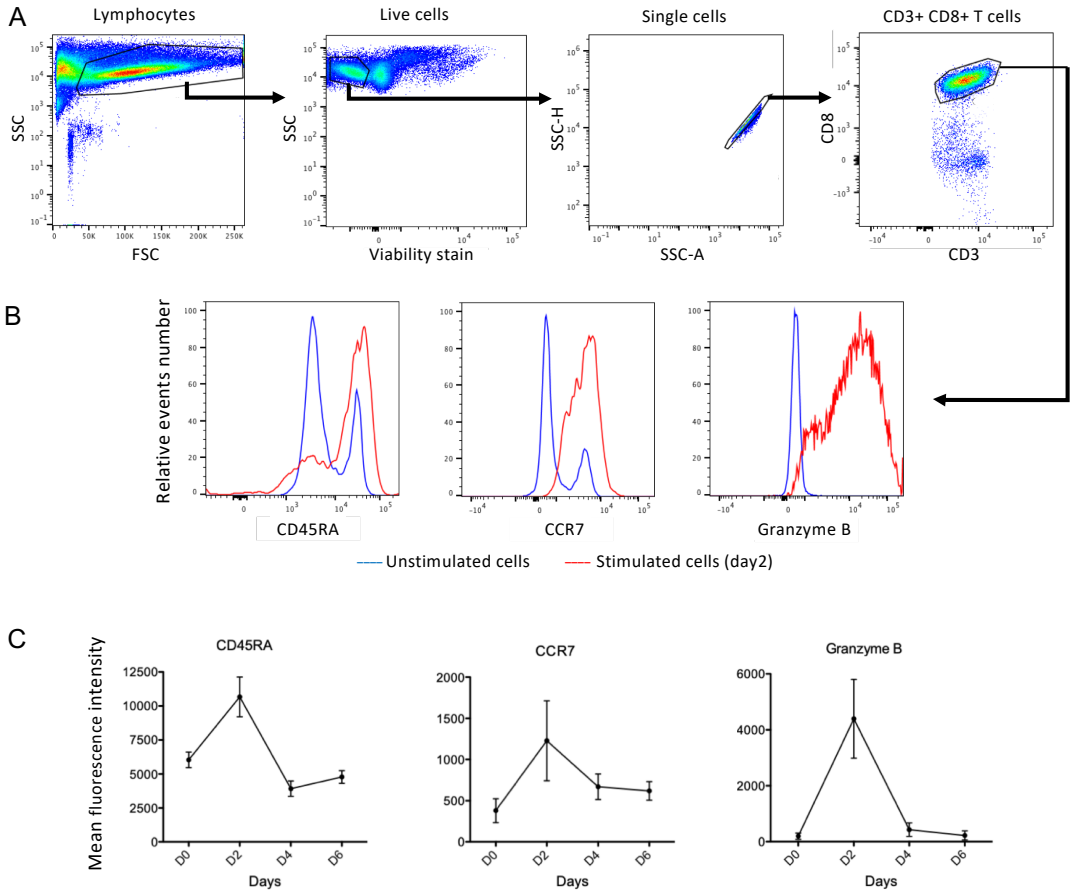

Figure 2. Expression of T cell molecules characteristic of human CTL differentiation.
Expression of CD45RA, CCR7 and granzyme B was analyzed by FACS in $CD3^{+}CD8^{+}$ T cells stimulated *ex vivo* with CD3+CD28 antibodies for the depicted number of days. At each time point, cells were stained with anti-CD3-PE-Cy5, anti-CD8-APC-Cy7, anti-CD45RA-APC, anti-CCR7-PE and anti-Granzyme-B-PE fluorescent antibodies.
(A): FACS gating strategy to measure single, live, CD3+CD8+ T cells.
(B): Histogram plots showing fluorescence intensity of CD45RA, CCR7 and granzyme B CTL differentiation markers in CD8+ T cells after 2 days of stimulation.
(C): Time course of differentiation marker expression upon CD3+CD28 stimulation. Mean florescence intensity versus time (Mean ± SEM, n= 8 healthy donors).

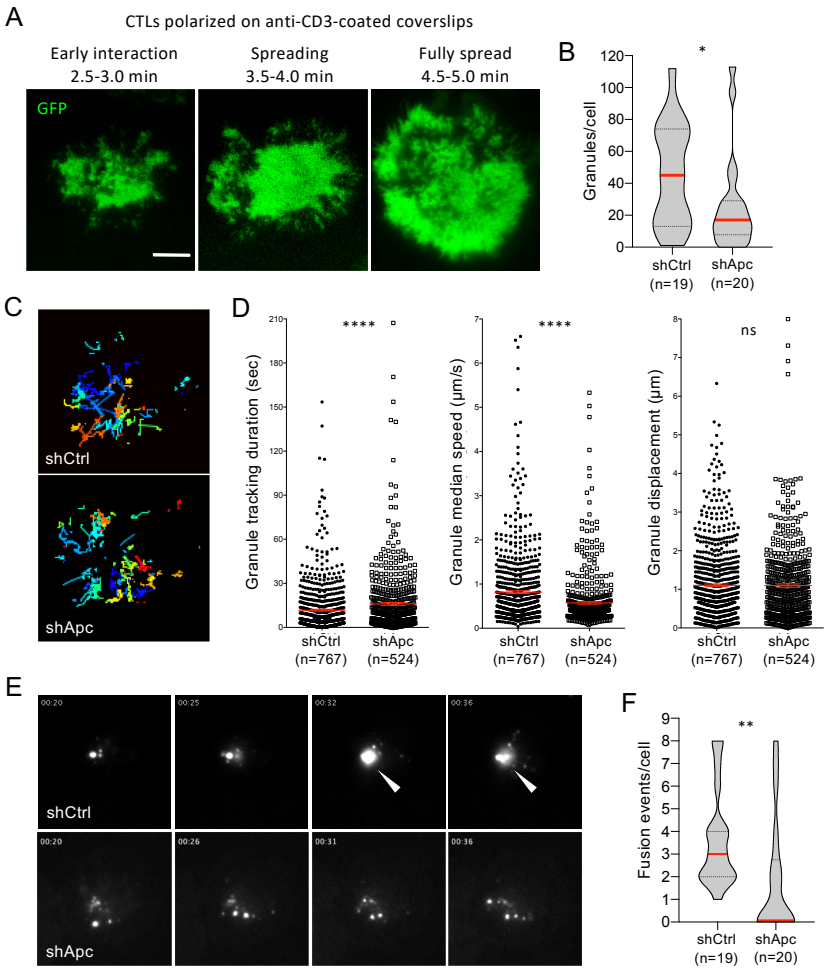

Figure 3. Quantifying granule secretion by human CTLs using TIRF microscopy. Effect of Apc silencing.
Ex vivo differentiated primary human CTLs were infected with control or APC shRNA lentiviral vectors expressing GFP, and selected with puromycin in culture. Previous to the assay, cells were incubated with LysoTracker to label lytic granules as part of the late endosomal-lysosomal compartment. Cells were set on anti-CD3-coated coverslips to form flat pseudo-immunological synapses and observed by TIRF microscopy.
(A): Cell spreading observed by GFP signal in the TIRF zone.(B): Detection of LysoTracker+ granules in the TIRF zone was used as a readout of granule-targeting events per synapse.
(C): Individual granule trajectories were obtained by fluorescent tracking of puncta.
(D): Tracking duration, average speed, and displacement length were assessed.
(E, F): Among the detected lytic granules, some made a fluorescence burst, indicative of fusion with the plasma membrane (arrowhead). The number of bursts was used as a readout of granule fusion events. Data reported in (Juzans et al., 2020).